

# Importance of instantaneous radiative forcing for rapid tropospheric adjustment

Tomoo Ogura · Mark J. Webb · Masahiro Watanabe ·  
F. Hugo Lambert · Yoko Tsushima · Miho Sekiguchi

Received: 1 June 2013 / Accepted: 23 September 2013 / Published online: 8 October 2013  
© Springer-Verlag Berlin Heidelberg 2013

**Abstract** To better understand CFMIP/CMIP inter-model differences in rapid low cloud responses to CO<sub>2</sub> increases and their associated effective radiative forcings, we examined the tropospheric adjustment of the lower tropospheric stability (LTS) in three general circulation models (GCMs): HadGEM2-A, MIROC3.2 medres, and MIROC5. MIROC3.2 medres showed a reduction in LTS over the sub-tropical ocean, in contrast to the other two models. This reduction was consistent with a temperature decrease in the mid-troposphere. The temperature decrease was mainly driven by instantaneous radiative forcing (RF) caused by an increase in CO<sub>2</sub>. Reductions in radiative and latent heating, due to clouds, and in adiabatic and advective heating, also contribute to the temperature decrease. The instantaneous RF in the mid-troposphere in MIROC3.2 medres is inconsistent with the results of line-by-line (LBL) calculations, and thus it is considered questionable.

These results illustrate the importance of evaluating the vertical profile of instantaneous RF with LBL calculations; improved future model performance in this regard should help to increase our confidence in the tropospheric adjustment in GCMs.

**Keywords** Tropospheric adjustment · Radiative forcing · Climate sensitivity · General circulation model · Lower tropospheric stability

## 1 Introduction

Equilibrium climate sensitivity estimates from general circulation models (GCMs) exhibit considerable spread (Randall et al. 2007). Radiative forcing (RF) due to increasing atmospheric CO<sub>2</sub> is one of the factors contributing to that spread. For example, effective RF caused by CO<sub>2</sub> doubling, which is estimated by the multi-model ensemble experiments coordinated by the Coupled Model Intercomparison Project—Phase 3 (CMIP3) and the Cloud Feedback Model Intercomparison Project—Phase 1 (CFMIP1), gives the range of 1.5 W/m<sup>2</sup>, from 3.0 to 4.5 W/m<sup>2</sup> (Webb, Lambert and Gregory 2013, hereafter WLG13). The estimated range of the effective RF when CO<sub>2</sub> quadruples amounts to 3.4 W/m<sup>2</sup>, from 5.2 to 8.6 W/m<sup>2</sup>, according to the analysis of the CMIP5 multi-model ensemble (Andrews et al. 2012). Those estimates from CMIP3/CFMIP1 and CMIP5 correspond to a climate sensitivity range on the order of 1.5 K, assuming a climate feedback of  $-1.08$  W/m<sup>2</sup>/K from the CMIP5 ensemble average (Andrews et al. 2012). It represents 58 % of the climate sensitivity range in the CMIP5 ensemble, which is 2.6 K, from 2.1 to 4.7 K (Andrews et al. 2012). RF is thus considered important for understanding inter-model

---

T. Ogura (✉)  
National Institute for Environmental Studies, 16-2 Onogawa,  
Tsukuba, Ibaraki 305-8506, Japan  
e-mail: ogura@nies.go.jp

M. J. Webb · Y. Tsushima  
Met Office Hadley Centre, FitzRoy Road, Exeter EX1 3PB, UK

M. Watanabe  
Atmosphere and Ocean Research Institute, The University of  
Tokyo, 5-1-5 Kashiwanoha, Kashiwa, Chiba 277-8568, Japan

F. H. Lambert  
College of Engineering, Mathematics and Physical Sciences,  
University of Exeter, Harrison Building, North Park Road,  
Exeter EX4 4QF, UK

M. Sekiguchi  
Tokyo University of Marine Science and Technology,  
2-1-6 Etchujima, Koto-ku, Tokyo 135-8533, Japan

differences in estimated climate sensitivity, although its contribution to the spread is not as large as the climate feedback (WLG13).

The spread in effective RF comes from various factors including differences among models in cloud response to CO<sub>2</sub> increase. Recent studies show that, in response to an abrupt CO<sub>2</sub> increase, there are rapid changes in clouds prior to any increase in globally averaged surface air temperature (Gregory and Webb 2008; Andrews and Forster 2008). The cloud changes are a response to heating induced by the CO<sub>2</sub> increase and are considered part of a tropospheric adjustment that occurs over time scales of days to weeks (Hansen et al. 2005; Dong et al. 2009; Kamae and Watanabe 2012a). The rapid cloud changes, which we call ‘cloud adjustments’ hereafter, are not related to an increase in globally-averaged surface air temperature. Therefore, their impact on radiation at the top of the atmosphere (TOA) is not classified as a feedback but as a RF that, specifically, is connected to clouds. The cloud component of the effective RF can be evaluated with several methods, including one for calculating the change in cloud radiative effect (CRE) which is defined as the difference in the radiative fluxes between all-sky and clear sky (Charlock and Ramanathan 1985). There is another method using the cloud radiative kernel technique (Zelinka et al. 2012) which allows more accurate calculation of the cloud component than using the CRE. The cloud component of the effective RF evaluated by the CRE (WLG13; Andrews et al. 2012) and the cloud radiative kernel technique (Zelinka et al. 2013) both exhibit a large spread among the models, suggesting that cloud adjustments are important to inter-model differences in effective RF. In particular, the region over low latitude oceans (30°S–30°N) shows a larger spread compared to other regions in the CMIP3/CFMIP1 ensemble (WLG13). Hence, we focus on this region in the following discussion.

The mechanism of the cloud adjustment to CO<sub>2</sub> increase has been discussed in previous studies. Using a version of the Australian Bureau of Meteorology Research Centre climate model, Colman and McAvaney (2011) found that cloud fraction decreases in the lower to middle troposphere due to a decreased relative humidity, which is related to enhanced heating rates and a temperature rise caused by the CO<sub>2</sub> increase. In the Model for Interdisciplinary Research on Climate—Version 5 (MIROC5), Kamae and Watanabe (2012a) noted a downward shift of marine boundary layer clouds. This feature is consistent with the increased static stability in the lower troposphere due to temperature rise induced by the direct effect of CO<sub>2</sub> increase. Wyant et al. (2012) also found a shallowing of the subtropical marine boundary layer associated with reduced entrainment through the trade inversion, using a superparameterized climate model (SP-CAM) and a two-dimensional cloud-

resolving model. Recently, cloud adjustments in the CMIP5 multi-model ensemble were examined by Kamae and Watanabe (2012b). Total cloud amount reduces in most of the CMIP5 ensemble members, but the spread in the magnitude of the changes is considerable. The mechanisms controlling the magnitude remain to be clarified.

Understanding the inter-model spread in cloud adjustment may be assisted by looking at such measures as lower tropospheric stability (LTS, Klein and Hartmann 1993). The LTS, defined as the difference in potential temperature between 700 hPa and sea surface, is highly correlated with subtropical stratus cloud amount with respect to seasonal, inter-regional, and inter-annual variation in the present climate (Klein and Hartmann 1993). An alternative measure is estimated inversion strength (EIS) which has an even higher correlation with stratus cloud amount than LTS (Wood and Bretherton 2006). We expect that LTS and EIS measure how well the environment (namely, the static stability or the strength of the inversion capping the planetary boundary layer) is favorable for maintaining the low cloud. Response of those measures to CO<sub>2</sub> increase will indicate the changes in the environment that lead to cloud adjustment.

There are several pieces of evidence which support the above argument. Firstly, the cloud components of effective RF induced by CO<sub>2</sub> doubling in the CMIP3/CFMIP1 ensemble are strongly anti-correlated with the EIS responses in the stable regime (WLG13). This feature suggests a relationship between the magnitude of changes in inversion strength and in low stratus cloud amount. Secondly, cloud responses are found to be consistent, although to a limited extent, with the LTS response in both the perturbed SST experiment using the SP-CAM superparameterized climate model (Wyant et al. 2009) and the CO<sub>2</sub> quadrupling experiment using MIROC5 (Watanabe et al. 2012). LTS or EIS may be a useful measure to understand inter-model spread in low cloud adjustment. In the present study, we focus mainly on the LTS because it is a simpler diagnostic than the EIS, which makes the understanding of the inter-model spread less complicated.

The LTS adjustment to an increase in CO<sub>2</sub> exhibits considerable spread among the GCMs. WLG13 estimated LTS adjustments in the CMIP3/CFMIP1 ensemble and found that most of the models show an increase in LTS. However, one model, MIROC3.2 medres, shows a substantial decrease in LTS, the mechanism of which is still uncertain (Figure 9d in WLG13). This behaviour of MIROC3.2 medres requires further investigation because it is the primary cause of the inter-model spread of the LTS adjustment in the CMIP3/CFMIP1 ensemble. In addition, the decrease in LTS is inconsistent with the current understanding of cloud adjustment, which suggests that temperature should increase in the lower to middle troposphere and cause an increase in the LTS (Colman and

McAvaney 2011; Kamae and Watanabe 2012a). We also note that the LTS decrease in MIROC3.2 medres is pronounced in the most stable regime in the low latitude oceans, accompanied by the large increase in shortwave (SW) cloud component of the effective RF, which is suggestive of low cloud decrease (WLG13). Hence, the LTS decrease may also be the key to understanding the large effective RF of MIROC3.2 medres, one of the largest in the CMIP3/CFMIP1 ensemble (WLG13). What is the origin of the negative LTS adjustment to CO<sub>2</sub> increase in MIROC3.2 medres? Is the process involved physically plausible, or is it indicative of some model deficiency that requires correction? These are the questions addressed in this study. This study has several implications for the tropospheric adjustments in the CMIP/CFMIP ensembles. Especially, the importance of instantaneous RF for the LTS and cloud adjustments will be illustrated.

We organize the remainder of this paper as follows: Sect. 2 describes the models used and the design of numerical experiments; Sect. 3 reports on the output of the numerical experiments and discusses the mechanism of the modelled LTS adjustments; and Sect. 4 summarizes results and discusses their meaning in relation to the inter-model spread in CO<sub>2</sub>-induced RF.

## 2 Models and experimental design

The three GCMs used for this study are MIROC3.2 medres (Hasumi and Emori 2004), MIROC5 (Watanabe et al. 2010), and the Hadley Centre Global Environmental Model version 2-A (HadGEM2-A; Bellouin et al. 2007; Collins et al. 2008). MIROC3.2 medres and MIROC5 are coupled ocean–atmosphere GCMs that contribute to CMIP3 and CMIP5, respectively. We only used the atmospheric components of the two models for this study. MIROC3.2 medres was jointly developed at the Center for Climate System Research (CCSR), the University of Tokyo, the National Institute for Environmental Studies (NIES), and the Japan Agency for Marine–Earth Science and Technology (JAMSTEC). It has a resolution of T42 (2.8° × 2.8°) with 20 vertical levels in the atmosphere. MIROC5 is the updated version of MIROC3.2 medres with improved representations of radiation, cumulus convection, cloud, turbulence, and aerosol transport. The resolution in the atmosphere is T85 (1.4° × 1.4°) with 40 vertical levels. HadGEM2-A, developed at the Met Office Hadley Centre, is the atmospheric component of the Earth System Model, HadGEM2-ES. It has a resolution of N96 (1.875° × 1.25°) with 38 vertical levels. HadGEM2-A and HadGEM2-ES both contribute to CMIP5.

To evaluate tropospheric adjustment to an increase in CO<sub>2</sub> in the three GCMs, we conducted ‘AMIP’ and ‘AMIP4xCO<sub>2</sub>’ CFMIP2 experiments according to the CMIP5 protocol (experiments 3.3 and 6.5 described by Taylor et al. 2009). For boundary conditions, we imposed SST and sea ice cover based on observations to the three GCMs, following Taylor et al. (2000), and ran the models for 30 years from 1979 to 2008. In the AMIP4 × CO<sub>2</sub> experiment, CO<sub>2</sub> is set four times higher than in the AMIP experiment. RF and tropospheric adjustment due to a CO<sub>2</sub> quadrupling were evaluated by subtracting the AMIP run from the AMIP4 × CO<sub>2</sub> run, following Hansen et al. (2005). We used the average over 30 years for the analysis.

As shown later in Sect. 3, we discuss relatively small responses to CO<sub>2</sub> quadrupling in MIROC3.2 medres. Therefore, the statistical significance of the responses was tested by running four members of the ensemble starting from different initial conditions. We confirmed in a *t* test that the discussed responses were significant at the 95 % confidence level. As for MIROC5 and HadGEM2-A, we conducted only one member for each experiment.

There are two commonly-used options for evaluating tropospheric adjustment: one is the regression method by Gregory and Webb (2008), and the other is the fixed SST methodology by Hansen et al. (2005). Previous studies point out that the tropospheric adjustments evaluated by the two methods are not exactly the same because the definition of the adjustment is different between the methods (Gregory and Webb 2008; Bala et al. 2010). For example, the fixed SST method evaluates the forcing consistent with a land surface temperature response which has equilibrated in response to the CO<sub>2</sub> increase, while the regression method evaluates a forcing consistent with a global mean near surface temperature response of zero. For this study, as described above, we adopted the fixed SST method with the AMIP boundary condition. This step was taken to confirm the results of WLG13 who took the regression approach. The results in this study clarify whether the negative LTS adjustment of MIROC3.2 medres, as described in the Introduction, is a robust feature which we observe with both methods.

We also note that the three selected GCMs are suitable for studying the LTS adjustment because they serve as good examples to compare adjustments with different signs. As shown later, MIROC5 and HadGEM2-A give positive LTS responses, which are different from that of MIROC3.2 medres. In addition, MIROC5, as an updated version of MIROC3.2 medres, informs us about the impact of model improvement on the simulated tropospheric adjustment.

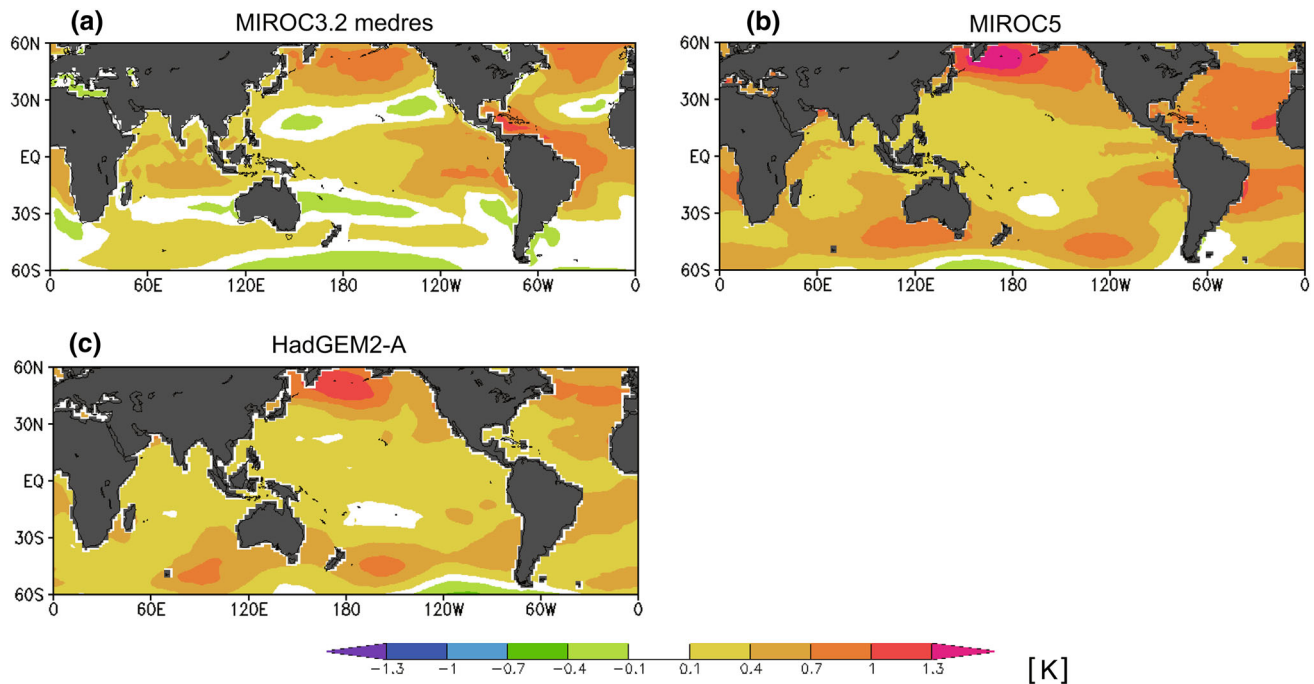


**Fig. 1** Annual mean LTS response to CO<sub>2</sub> quadrupling: **a** MIROC3.2 medres, **b** MIROC5, and **c** HadGEM2-A

### 3 Tropospheric adjustment diagnosed from fixed SST experiments

#### 3.1 Intercomparison of GCMs

The LTS response to CO<sub>2</sub> quadrupling is shown over the ocean for MIROC3.2 medres, MIROC5, and HadGEM2-A in Fig. 1. As expected, the response is mostly positive, because the potential temperature rises at 700 hPa with tropospheric radiative heating in response to the CO<sub>2</sub> increase, while it remains nearly constant at sea level due to the fixed-SST boundary conditions. If we focus on the subtropical ocean, however, we also find a negative response in MIROC3.2 medres, in contrast to the other two models. This feature is consistent with the LTS response estimated by the regression method in the previous study, which showed that the LTS decreased over the low latitude oceans in MIROC3.2 medres while it increased in the other CMIP3/CFMIP1 models (WLG13).

Figure 2 shows the response of the EIS as an alternative measure of the environment favourable for stratiform low cloud cover. The EIS is defined as

$$EIS = LTS - \Gamma_m^{850}(Z_{700} - LCL), \quad (1)$$

where  $\Gamma_m^{850}$  is the moist adiabat at 850 hPa,  $Z_{700}$  is the height of the 700 hPa surface, and  $LCL$  is the lifting condensation level (Wood and Bretherton 2006). In MIROC3.2 medres, negative response predominates over the subtropical ocean, especially on the eastern side of the

ocean basins. MIROC5 and HadGEM2-A, on the other hand, show positive responses more often than negative. This confirms the results of the EIS adjustment estimated with the regression method by WLG13, who showed that EIS decreases in MIROC3.2 medres while it increases in most other CMIP3/CFMIP1 models. We also note that the negative EIS responses correspond to the negative LTS responses over the subtropics in MIROC3.2 medres (Figs. 1a, 2a). The negative LTS response is thus a contributing factor to the negative EIS response, according to the definition of the EIS in Eq. (1).

Next we discuss how the LTS and EIS are related to the effective RF. Figure 3 shows the response of the net cloud radiative effect (NCRE) to CO<sub>2</sub> quadrupling. We estimated the cloud-masking bias and removed it from the NCRE response before displaying in Fig. 3, which makes the NCRE response a better measure of the radiative effect of cloud changes (Soden et al. 2004). The cloud-masking bias is estimated by double radiation calculations; namely, we repeat the radiative transfer calculation with  $1 \times \text{CO}_2$  and  $4 \times \text{CO}_2$  conditions in the control simulation, and estimate the change in CRE which is caused solely by CO<sub>2</sub> quadrupling without any change in cloud (Wyant et al. 2012). In Fig. 3, the positive response of NCRE tends to increase the effective RF of CO<sub>2</sub> quadrupling. Among the three models, MIROC3.2 medres shows the largest positive response, especially over subtropical oceans. The inter-model differences over the subtropical oceans are reflected in the regional average equatorward of 60°S and 60°N, which are

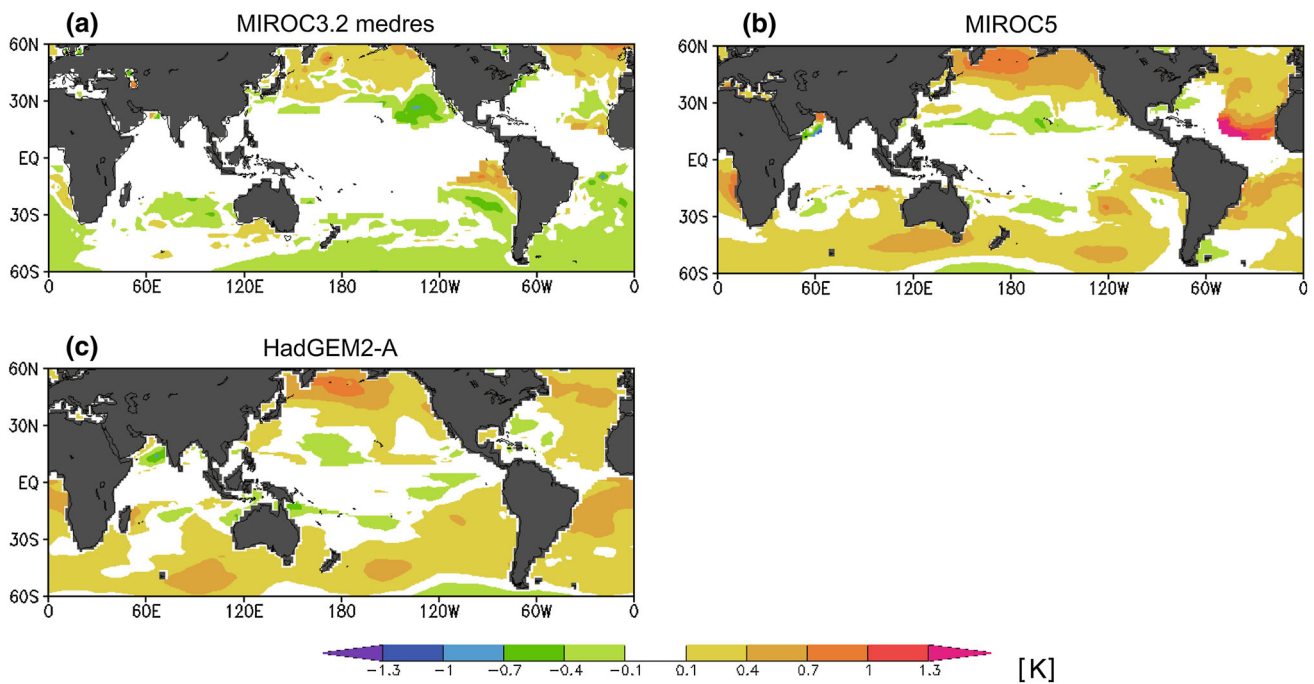


**Fig. 2** Annual mean EIS response to CO<sub>2</sub> quadrupling: **a** MIROC3.2 medres, **b** MIROC5, and **c** HadGEM2-A

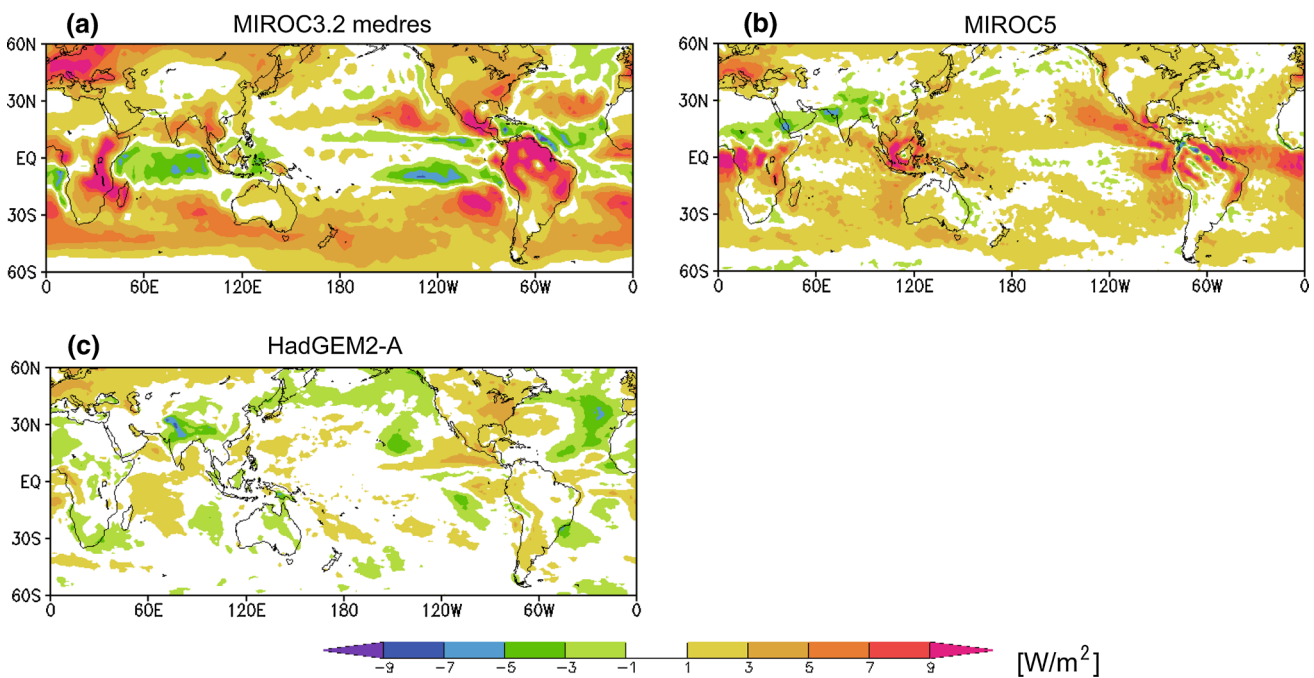


**Fig. 3** Annual mean NCRE response to CO<sub>2</sub> quadrupling: **a** MIROC3.2 medres, **b** MIROC5, and **c** HadGEM2-A

2.0, 1.5, and 0.0 (W/m<sup>2</sup>) for MIROC3.2 medres, MIROC5, and HadGEM2-A, respectively (Table 1). The inter-model difference in the NCRE response appears consistent with that in the EIS response; namely, the large positive response of NCRE in MIROC3.2 medres corresponds to the decrease in EIS, while smaller positive (or negative) response of the NCRE in MIROC5 and HadGEM2-A, compared to

MIROC3.2 medres, corresponds to the increase in EIS. The results obtained so far support the idea that inter-model difference in the effective RF is associated with the changes in the environment which favours stratiform low cloud cover, as measured by the EIS. The LTS is one of the key factors for understanding the different EIS responses among the three models, according to the Eq. (1).

**Table 1** Effective RF of CO<sub>2</sub> quadrupling at TOA in annual and regional average equatorward of 60°S and 60°N

Model	RF	CLR			CRE		
		NET	LW	SW	NET	LW	SW
MIROC3.2 medres	8.00	7.05	6.78	0.26	2.09 (−1.14)	−0.40 (−1.14)	2.50 (0.00)
MIROC5	9.23	9.15	8.91	0.23	1.56 (−1.48)	−0.58 (−1.51)	2.15 (0.03)
HadGEM2-A	6.89	7.78	7.84	−0.05	0.04 (−0.93)	−0.39 (−1.07)	0.44 (0.13)
Mean	8.04	7.99	7.84	0.14	1.23 (−1.18)	−0.45 (−1.24)	1.69 (0.05)
Standard deviation	0.95	0.87	0.86	0.13	0.86 (0.22)	0.08 (0.19)	0.90 (0.05)

The clear sky (CLR) and cloud (CRE) components are also shown with respect to net (NET), longwave (LW) and shortwave (SW) components. For the cloud components (CRE), we estimated the cloud masking bias and removed it from the CRE before displaying in the table. The cloud masking biases are indicated by parentheses. Units are in W/m<sup>2</sup>

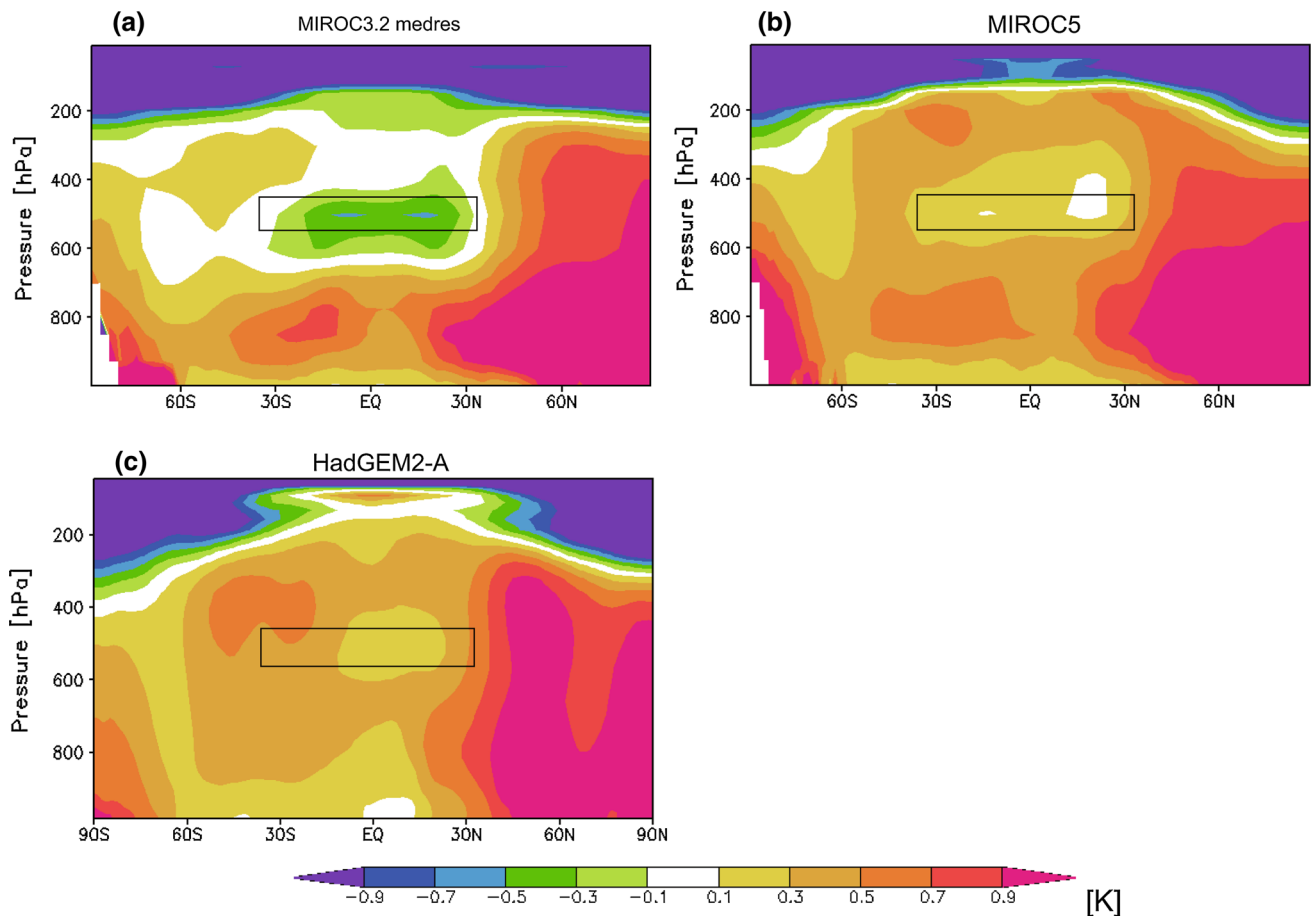


**Fig. 4** Zonal annual mean temperature response to CO<sub>2</sub> quadrupling: **a** MIROC3.2 medres, **b** MIROC5, and **c** HadGEM2-A. The black squares indicate the region of 36°S–33°N, 0°–360°E, and 550–450 hPa. They will be referred to in Figs. 5, 6 and 7

### 3.2 Processes contributing to inter-model difference

To illustrate how the LTS responds differently among the three models, we next look at the vertical temperature profile in Fig. 4. In MIROC3.2 medres, there is a temperature decrease in the mid-troposphere, which does not appear in the other two models. The negative temperature response extends down to 700 hPa over the subtropical

oceans, although it does not appear in the zonally averaged picture in Fig. 4a. This leads to a negative (or small positive) response of potential temperature at 700 hPa and a negative response of LTS in the subtropics, as shown in Fig. 1. Hence, the difference in LTS response between MIROC3.2 medres and the other two models appears to be linked to the difference in temperature response in the mid-troposphere.

We examined the mechanisms that lead to different temperature responses in the mid-troposphere and discuss first the negative response in MIROC3.2 medres. The temperature tendency equation in the three GCMs is:

$$\frac{\partial T}{\partial t} = LW + SW + CLD\_VDF + DYN + RSD, \tag{2}$$

where the terms on the right hand side are heating rates from longwave (LW) radiation, SW radiation, cloud and vertical eddy diffusion (CLD\_VDF), dynamics (DYN), and residual processes (RSD). The CLD\_VDF includes latent heating from condensation, evaporation, ice crystal growth from water vapour, and sublimation in convective and non-convective cloud parameterizations. It also includes the tendency from vertical mixing by turbulent eddies in the planetary boundary layer.

Integrating Eq. (2) from  $t = 0$  to  $t = 30$  years in the AMIP4  $\times$  CO<sub>2</sub> run, we obtain

$$\Delta T = (\overline{LW} + \overline{SW} + \overline{CLD\_VDF} + \overline{DYN} + \overline{RSD}) \times \Delta t, \tag{3}$$

where  $\Delta X \equiv X_{t=30\text{year}} - X_{t=0\text{year}}$ ,  $\overline{X} = \int_{t=0}^{t=30\text{year}} X dt / \Delta t$ , and  $X$  is an arbitrary variable. If we take the initial condition of the AMIP4  $\times$  CO<sub>2</sub> run to be the same as the AMIP run, i.e. the simulated state of January 1st in the year 1979 with the  $1 \times$  CO<sub>2</sub> condition, then  $\Delta T$  corresponds to the temperature response due to CO<sub>2</sub> quadrupling in the AMIP4  $\times$  CO<sub>2</sub> run. Each term on the right hand side of Eq. (3) comprises a control state plus a response to CO<sub>2</sub> increase, such as  $\overline{LW} = \overline{LW}_{1 \times CO_2} + \delta \overline{LW}$  where  $\delta X \equiv X_{4 \times CO_2} - X_{1 \times CO_2}$ . We assume a balance of the tendency terms in the 30 year average of the control state as,

$$\overline{LW}_{1 \times CO_2} + \overline{SW}_{1 \times CO_2} + \overline{CLD\_VDF}_{1 \times CO_2} + \overline{DYN}_{1 \times CO_2} + \overline{RSD}_{1 \times CO_2} \approx 0. \tag{4}$$

Combining (3) and (4) gives

$$\Delta T = (\delta \overline{LW} + \delta \overline{SW} + \delta \overline{CLD\_VDF} + \delta \overline{DYN} + \delta \overline{RSD}) \times \Delta t. \tag{5}$$

Note that the LW term can be expressed as the sum of instantaneous RF,  $\overline{F_{i-LW}}$ , and rapid adjustment to CO<sub>2</sub> quadrupling,  $\overline{LW_{adj}}$ :

$$\delta \overline{LW} = \overline{F_{i-LW}} + \overline{LW_{adj}}. \tag{6}$$

In Eq. (6), the instantaneous forcing  $\overline{F_{i-LW}}$  is evaluated by a separate double radiation calculation. The adjustment term,  $\overline{LW_{adj}}$ , is obtained by subtracting  $\overline{F_{i-LW}}$  from the LW response,  $\delta \overline{LW}$ .

Combining Eqs. (5) and (6) gives

$$\Delta T = (\overline{F_{i-LW}} + \overline{LW_{adj}} + \delta \overline{SW} + \delta \overline{CLD\_VDF} + \delta \overline{DYN} + \delta \overline{RSD}) \times \Delta t. \tag{7}$$

The temperature response  $\Delta T$  is now related to the instantaneous RF, the LW adjustment, and the time-averaged tendency responses on the right hand side of Eq. (7). Hence, we can examine the contribution of each term to the temperature response  $\Delta T$ .

The contribution of the terms on the right hand side of Eq. (7), after dividing them by  $\Delta t$ , is shown for MIROC3.2 medres in Fig. 5. Focusing on the region showing a distinct temperature decrease and highlighted by a black square, we notice that the largest contribution to cooling is from the LW instantaneous forcing,  $\overline{F_{i-LW}}$ . There are also smaller and localized negative contributions from SW, CLD\_VDF, and DYN. On the other hand,  $\overline{LW_{adj}}$  tends to oppose the temperature decrease. In some regions, CLD\_VDF and DYN also oppose the cooling. The small contribution to the cooling from SW and CLD\_VDF comes from the upper tip of the negative value in the lower troposphere around 600–800 hPa. The negative value reflects a reduced heating by SW absorption and by condensation of water vapour, both of which are consistent with the cloud decrease in the lower troposphere (not shown). The contribution of DYN appears consistent with the weakening of tropical circulation and the reduced adiabatic compression in its descending branch.

We also compared the instantaneous LW forcing among the three models (Fig. 6), focusing again on the mid-troposphere region indicated by the black square. Results indicate that the inter-model difference in the forcing is consistent with that in the temperature response, namely, the negative forcing corresponds to cooling in MIROC3.2 medres (Figs. 4a, 6a), the positive forcing corresponds to warming in HadGEM2-A (Figs. 4c, 6c), and the small positive forcing corresponds to a little warming in MIROC5 (Figs. 4b, 6b).

In addition, we considered if other temperature tendency terms are responsible for the temperature changes, following the Eq. 7. Results are summarized in Fig. 7 and indicate that except for the instantaneous LW forcing term, no term is fully consistent with the temperature responses of the three models. We note that the SW term shows some resemblance to temperature response, but its magnitude is much smaller than that of instantaneous LW forcing. The SW term cannot explain the negative temperature response of MIROC3.2 medres.

The evidence presented so far supports the idea that the instantaneous LW forcing is mainly responsible for the inter-model differences in the mid-tropospheric temperature response. Adjustment of other processes, such as

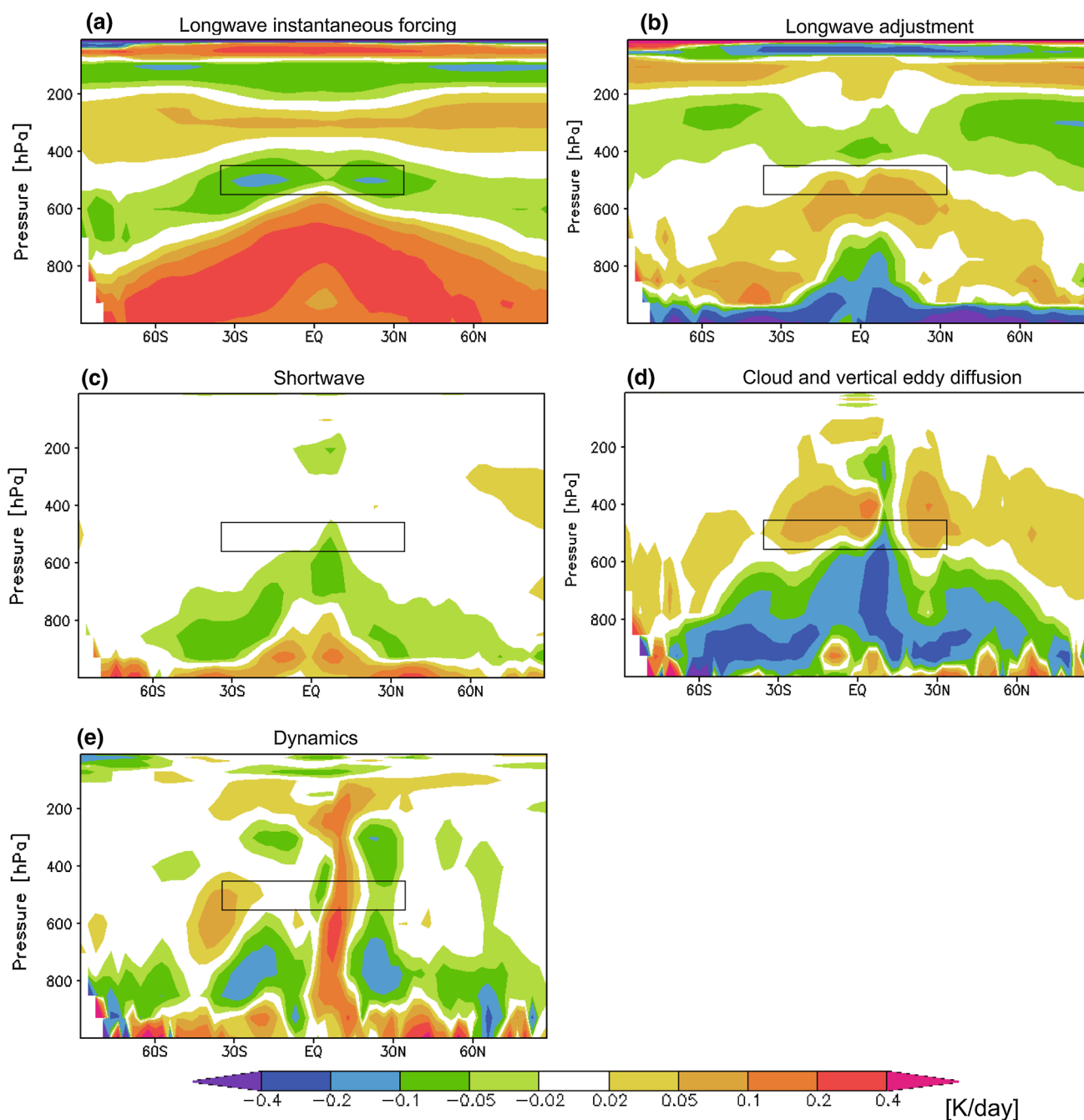


**Fig. 5** Zonal annual mean forcing and response of temperature tendency due to CO<sub>2</sub> quadrupling for MIROC3.2 medres: **a** LW instantaneous forcing, **b** LW rapid adjustment, **c** SW response, **d** CLD\_VDF response, and **e** DYN response. The *black squares* are as indicated in Fig. 4

radiative, latent, and adiabatic heatings, also makes some contribution, but the influence of these processes does not dominate in the focused region. Next, we discuss why the instantaneous LW forcing looks different among the three models despite application of the same atmospheric CO<sub>2</sub> increase. One possibility is that the simulated climate conditions (e.g. clouds) in the control experiments are different among the models, which would make the instantaneous LW forcings divergent.

To evaluate the impact of different cloud distributions in the control climates, we compared the clear sky component of the instantaneous LW forcing among the models, as shown in Fig. 8a. Note that the output of the three GCMs is averaged over 30°N–60°N for June July August, and multiplied by 0.52 for later comparison with the results of CO<sub>2</sub> doubling in Fig. 8b. The scaling factor of 0.52 is the ratio between TOA radiative forcings of CO<sub>2</sub> doubling and quadrupling in MIROC3.2 medres. In Fig. 8a, the tendency

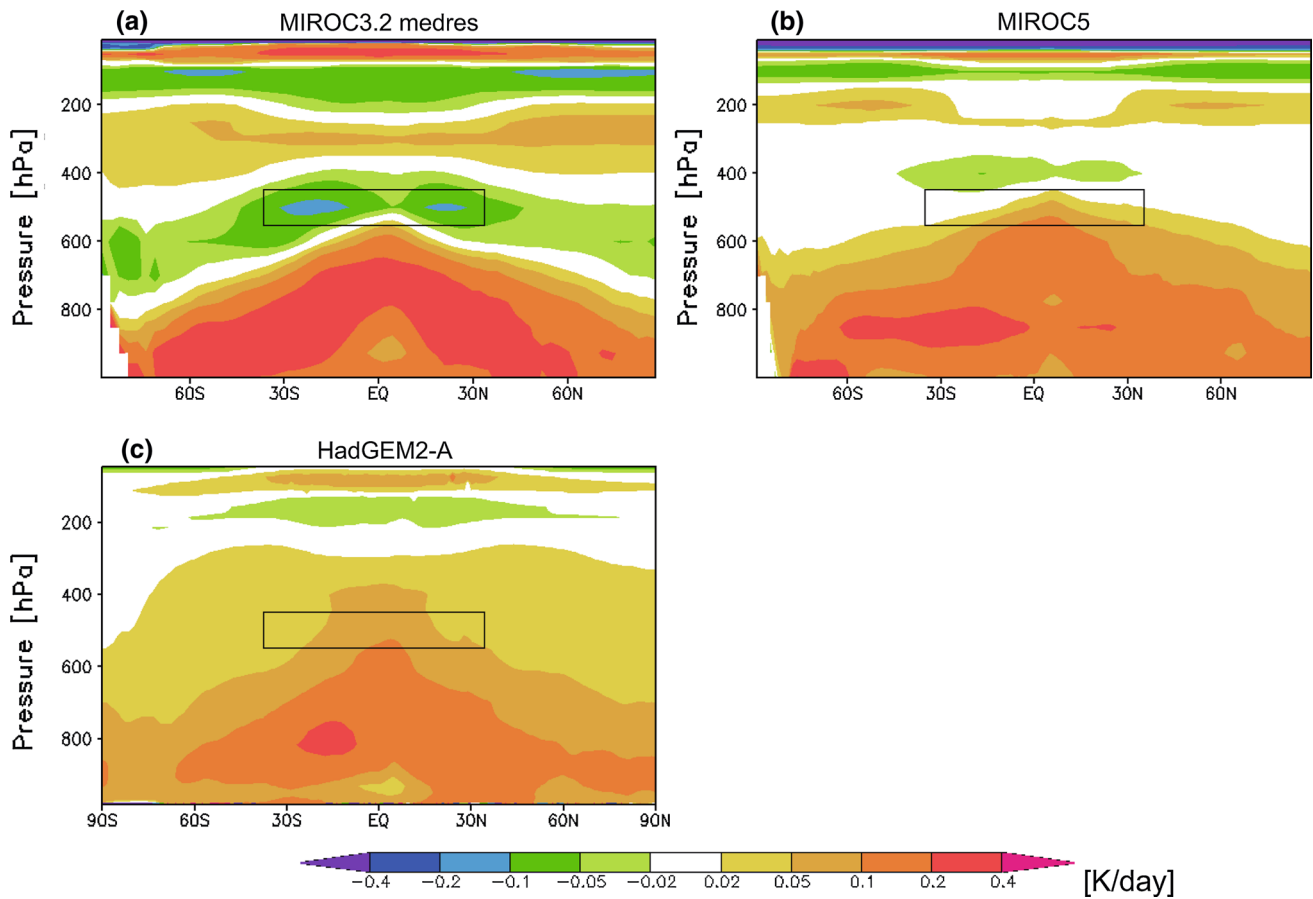


**Fig. 6** Zonal annual mean instantaneous LW forcing of CO<sub>2</sub> quadrupling: **a** MIROC3.2 medres, **b** MIROC5, and **c** HadGEM2-A. The *black squares* are as indicated in Fig. 4

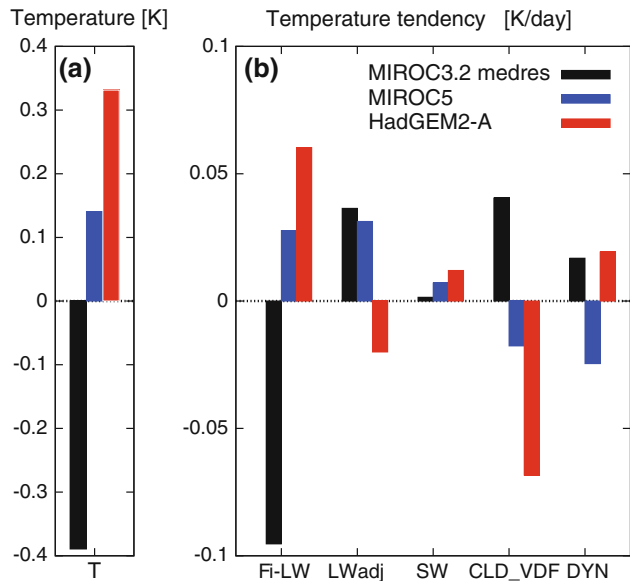


**Fig. 7** Response of **a** temperature and **b** temperature tendency terms averaged over the region indicated by the *black squares* in Figs. 4, 5, and 6. The temperature tendency response includes LW rapid adjustment (LWadj), SW, CLD\_VDF, and DYN. LW instantaneous forcing ( $\overline{F_{i-LW}}$ ) is also shown

to have a negative forcing in the mid-troposphere still persists for MIROC3.2 medres, in contrast to the other two models. This feature occurs even without the influence of clouds. The heating maximum around 800 hPa is also larger in MIROC3.2 medres compared to the other two models, a feature that is consistent with inter-model differences in the all-sky values (Fig. 6). Hence, we reject the idea that cloud distribution is the primary cause for the inter-model spread of the instantaneous LW forcing.

### 3.3 Intercomparison of radiation codes

To remove the effect of different climate conditions other than clouds on radiation calculations, we specified an identical vertical profile of temperature, water vapour, and ozone in the radiation codes used in the three GCMs. Then, we calculated the clear sky component of the instantaneous LW forcing of CO<sub>2</sub> doubling (Fig. 8b). The radiation codes used are MSTRN-8 for MIROC3.2 medres (Nakajima et al. 2000), MSTRN-X for MIROC5 (Sekiguchi and Nakajima 2008), and one based on Edwards and Slingo (1996) and Cusack et al. (1999) for HadGEM2-A. The calculation

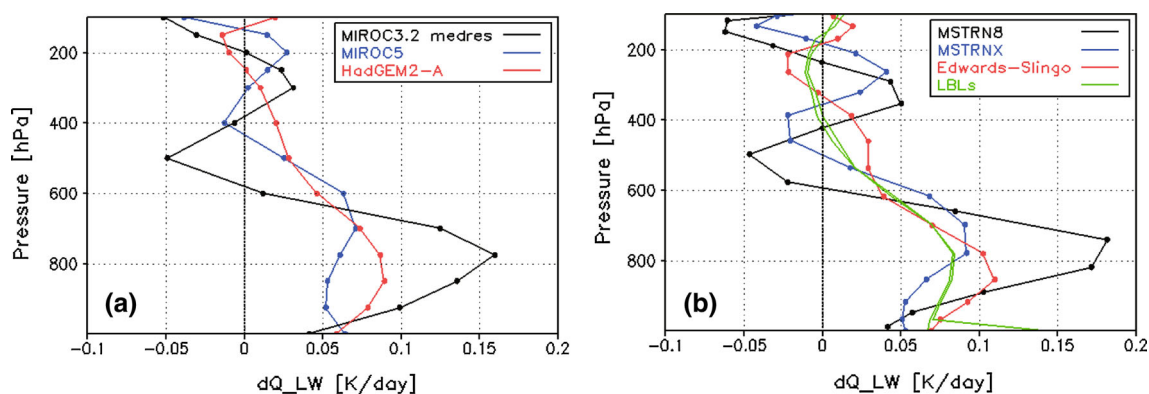


**Fig. 8** Instantaneous LW clear sky forcing of CO<sub>2</sub> doubling: **a** AMIP runs of GCMs averaged over 30°–60°N, JJA, and **b** GCM radiation codes and LBL calculations for the climatological mid-latitude summer atmospheric profile

protocol follows that of cases 2b and 1a from the Radiative Transfer Model Intercomparison Project (RTMIP; Collins et al. 2006). The background atmospheric state was defined as a climatological mid-latitude summer profile (Anderson et al. 1986).

The results using radiation codes with the same atmospheric profile are summarized in Fig. 8b and indicate that the inter-model differences that are seen among the three GCMs in Fig. 8a still appear. MSTRN-8 is the only code that shows a negative forcing in the mid-troposphere (500 hPa). The heating maximum in the lower troposphere (800 hPa) using this code for MIROC3.2 medres is much larger than the heating maxima found in the other models. Therefore, we surmise that differences in radiation codes, not in control climates, are responsible for the diversity of the instantaneous LW forcing.

The difference between the instantaneous LW forcing calculated by MSTRN-8 and MSTRN-X has been studied by Sekiguchi and Nakajima (2008). They concluded that the difference originates from three factors: (1) the database of line absorption parameters and the continuum absorption model, (2) absorption bands included in the model, and (3) the optimization method used to decrease the number of quadrature points for numerical integration in the correlated k-distribution method.

Finally, we examined which instantaneous LW forcing is more accurate than the others. As a reference, we plotted the forcing calculated by line-by-line (LBL) radiation codes in Fig. 8b; the forcing data was provided by Collins et al. (2006) at the RTMIP web site, <http://www.cgd.ucar.edu/RTMIP/>. The LBL codes are the most detailed models available for radiation calculations. They employ the most fundamental physics and evaluate the relevant equations with high numerical accuracy, providing benchmarks for testing less detailed parameterizations used in GCMs (Ellingson et al. 1991). The figure shows the results from two out of five LBL codes which participated in the RTMIP. The results of the remaining three LBL codes are similar to

the ones shown in Fig. 8b (Figure 10 in Collins et al. 2006). The LBL forcing shows a maximum heating in the lower troposphere around 800 hPa, which decreases in magnitude at higher altitudes. It also shows a cooling in the upper troposphere around 250 hPa. Considering the small spread among the LBL results, the negative forcing given by MSTRN-8 at the mid-troposphere around 500 hPa is not supported by the LBLs, and thus is considered questionable.

#### 4 Summary and discussion

The rapid adjustment of LTS to CO<sub>2</sub> quadrupling was evaluated using fixed-SST experiments (AMIP4 × CO<sub>2</sub> minus AMIP) and compared between three GCMs: MIROC3.2 medres, MIROC5, and HadGEM2-A. The MIROC3.2 medres is the only model showing an LTS decrease at low latitude oceans, which is consistent with a mid-tropospheric cooling. Analysis of temperature tendency terms indicates that the mid-tropospheric cooling is caused mainly by a negative instantaneous LW forcing induced by the CO<sub>2</sub> quadrupling in MIROC3.2 medres. Adjustment of radiative, latent, adiabatic and advective heatings makes a small contribution to the temperature decrease. The vertical profile of instantaneous LW forcing was also compared among the three GCMs. Results indicate that inter-model spread in the LW forcing stems from differences in radiation codes, rather than differences in atmospheric profiles among the models. The negative forcing given by MIROC3.2 medres in the mid-troposphere is not supported by LBL calculations, and hence is considered questionable.

The results of this study have several implications for the tropospheric adjustments in the CMIP/CFMIP ensembles. First, they provide an explanation for much of the inter-model spread of the LTS adjustment in the CMIP3/CFMIP1 ensemble. WLG13 point out that the inter-model

spread of the LTS adjustment occurs largely because MIROC3.2 medres has a characteristic negative response. The present study illustrates that the negative response can be traced back to the instantaneous LW forcing and that this forcing is inconsistent with results of LBL calculations. Hence, the inter-model spread of the LTS adjustment is expected to decrease considerably if we apply the LBL results as a constraint in GCM simulations.

We also note that the negative LTS response to CO<sub>2</sub> increase is inconsistent with the current understanding of tropospheric adjustment: a temperature rise in the lower troposphere that is induced by CO<sub>2</sub> increase, while keeping the surface air temperature fixed, will lead to an increase in LTS or equivalently, to a positive LTS adjustment. The present study shows that MIROC3.2 medres does not provide a plausible counter-example to that understanding; hence, the current understanding of tropospheric adjustment is not challenged.

Second, the present study brings about a better understanding of the high climate sensitivity of MIROC3.2 medres among the CMIP3/CFMIP1 ensemble. The climate sensitivity of MIROC3.2 medres is the third highest of the 12 models in the CMIP3/CFMIP1 ensemble, mainly due to its strong RF and especially forcing of the SW cloud component in lower and middle latitudes (WLG13). This feature presumably indicates that the low cloud decrease due to tropospheric adjustment is greater in MIROC3.2 medres than in the other models. The negative LTS adjustment of MIROC3.2 medres is suggested as one of the reasons for the significant decrease in low cloud (WLG13). The present study explains why the LTS adjustment is negative in MIROC3.2 medres. It also implies that MIROC3.2 medres would give a less negative LTS adjustment if instantaneous RF were made consistent with LBL results. A less negative LTS adjustment would also lead to smaller RF in MIROC3.2 medres and might reduce the inter-model spread in climate sensitivity in the CMIP3/CFMIP1 ensemble.

Third, this study shows that the vertical profile of instantaneous LW forcing can be relevant to the inter-model spread of LTS and cloud adjustments. It also presents an example of evaluating the vertical profile by referring to the LBL results. Collins et al. (2006) found that there is an inter-model spread in the vertical profile of the instantaneous LW forcing induced by CO<sub>2</sub> doubling when the profile is calculated by the radiation codes of the CMIP3 models. The spread is on the order of 0.05 K/day in the lower to middle troposphere. The present study illustrates that the spread is important to the adjustment of temperature and LTS, as much as to change its sign, and presumably also to cloud adjustment and effective RF. To reduce the inter-model spread in the estimated climate sensitivity, it is imperative to increase the accuracy of LTS and cloud adjustments modelled by different GCMs. The

present study implies that improving the accuracy of the instantaneous LW forcing is relevant to that purpose. With regard to the three GCMs considered here, a major part of the inter-model spread of the instantaneous LW forcing stems from differences in radiation codes, rather than differences in atmospheric profiles of temperature, water vapour, and cloud. In such cases, evaluating the clear sky forcing computed by radiation codes of different GCMs referring to the LBL results, as in the case of RTMIP, would be particularly effective for improving the accuracy of LTS adjustment.

Last, this study highlights the importance of temperature tendency terms for understanding inter-model differences in climate sensitivity. In recent years, various tendency terms have been used as a tool for elucidating the mechanisms of model behaviour. For example, cloud condensate tendency terms have been employed to discuss mechanisms responsible for different cloud responses to CO<sub>2</sub> increase among GCMs (Ogura et al. 2008a, b). Temperature or humidity tendency terms have also been used to investigate mechanisms of cloud feedback (Zhang and Bretherton 2008; Webb and Lock 2012; Zhang et al. 2012) and model errors in short term weather prediction (Williamson et al. 2005; Rodwell and Palmer 2007; Williams and Brooks 2008). The present study provides another example illustrating the utility of the temperature tendency terms. The requested CFMIP2 variables in the CMIP5 experiments include a set of tendency terms related to cloud, temperature and water vapour (Bony et al. 2011). Analysis of those terms from the multi-model ensemble will assist in understanding inter-model spread in climate sensitivity.

There are also limitations to the above arguments. It remains to be seen whether the processes suggested in this study, in which the instantaneous LW forcing causes the inter-model spread in temperature and LTS adjustments, is still relevant for the latest multi-model ensemble of CMIP5/CFMIP2. Improvements in radiation codes may have reduced the inter-model spread in the instantaneous LW forcing in CMIP5/CFMIP2 compared to CMIP3/CFMIP1. For example, the MSTRN-X used in MIROC5 performs better than its predecessor MSTRN-8 in MIROC3.2 in reproducing the LBL results. The problem of mid-tropospheric cooling appears alleviated by the model update. Whether the instantaneous LW forcing is important to the inter-model spread, even with the current updates in the radiation codes, is still uncertain.

We also note that the most important factor contributing to the inter-model spread in climate sensitivity is not the RF but climate feedback (WLG13). Therefore, improving the accuracy of climate feedback, as well as the tropospheric adjustment included in the RF, is imperative to reduce the spread.

Still, there remains the possibility that errors in instantaneous RF contribute to the inter-model spread of climate sensitivity in the CMIP5/CFMIP2 ensemble. To examine if this is the case, instantaneous RF of the ensemble members needs to be investigated and should be the subject of future study.

**Acknowledgments** We acknowledge the Radiative Transfer Model Intercomparison Project (RTMIP) for providing atmospheric profile and LBL data and the Atmospheric Radiation Measurement (ARM) Program for distributing the RTMIP data. We also acknowledge two anonymous reviewers for their constructive and insightful comments on the manuscript. This work was supported by the Program for Risk Information on Climate Change from the Ministry of Education, Culture, Sports, Science and Technology, Japan. This work was also supported by JSPS KAKENHI Grant Number 23310014 and 23340137. The contribution to this work from the Hadley Centre was supported by the Joint DECC/Defra Met Office Hadley Centre Climate Programme (GA01101) and funding from the European Union, Seventh Framework Programme (FP7/2007–2013), under Grant Agreement Number 244067 via the EU CLOUD Intercomparison and Process Study Evaluation Project (EUCLIPSE). The Earth Simulator at JAMSTEC and the NEC SX-8R/128M16 at NIES were used to carry out the model simulations.

## References

- Anderson GP, Clough SA, Kneizys FX, Chetwynd JH, Shettle EP (1986) AFGL atmospheric constituent profiles (0–120 km), Tech Rep AFGL-TR-86-0110, Air Force Geophys Lab, Hanscom Air Force Base, MA
- Andrews T, Forster PM (2008) CO<sub>2</sub> forcing induces semi-direct effects with consequences for climate feedback interpretations. *Geophys Res Lett* 35:L04802. doi:10.1029/2007GL032273
- Andrews T, Gregory JM, Webb MJ, Taylor KE (2012) Forcing, feedbacks and climate sensitivity in CMIP5 coupled atmosphere–ocean climate models. *Geophys Res Lett* 39:L09712. doi:10.1029/2012GL051607
- Bala G, Caldeira K, Nemani R (2010) Fast versus slow response in climate change: implications for the global hydrological cycle. *Clim Dyn* 35:423–434. doi:10.1007/s00382-009-0583-y
- Bellouin N, Boucher O, Haywood J, Johnson C, Jones A, Rae J, Woodward S (2007) Improved representation of aerosols for HadGEM2. Hadley Centre Tech Note 73, p 43
- Bony S, Webb MJ, Bretherton CS, Klein SA, Siebesma P, Tselioudis G, Zhang M (2011) CFMIP: towards a better evaluation and understanding of clouds and cloud feedbacks in CMIP5 models. *CLIVAR Exch* 56, 16(2):20–24
- Charlock TP, Ramanathan V (1985) The albedo field and cloud radiative forcing produced by a general circulation model with internally generated cloud optics. *J Atmos Sci* 42(13):1408–1429
- Collins WD, Ramaswamy V, Schwarzkopf MD, Sun Y, Portmann RW, Fu Q, Casanova SEB, Dufresne JL, Fillmore DW, Forster PMD, Galin VY, Gohar LK, Ingram WJ, Kratz DP, Lefebvre MP, Li J, Marquet P, Oinas V, Tsushima Y, Uchiyama T, Zhong WY (2006) Radiative forcing by well-mixed greenhouse gases: estimates from climate models in the intergovernmental panel on climate change (IPCC) fourth assessment report (AR4). *J Geophys Res* 111:D14317. doi:10.1029/2005JD006713
- Collins WJ, Bellouin N, Doutriaux-Boucher M, Gedney N, Hinton T, Jones CD, Liddicoat S, Martin G, O'Connor F, Rae J, Senior C, Totterdell I, Woodward S, Reichler T, Kim J (2008) Evaluation of the HadGEM2 model. Hadley Centre Tech Note 74, p 47
- Colman RA, McAvaney BJ (2011) On tropospheric adjustment to forcing and climate feedbacks. *Clim Dyn* 36:1649–1658. doi:10.1007/s00382-011-1067-4
- Cusack S, Edwards JM, Crowther JM (1999) Investigating k-distribution methods for parameterizing gaseous absorption in the Hadley Centre climate model. *J Geophys Res* 104:2051–2057
- Dong B, Gregory JM, Sutton RT (2009) Understanding land-sea warming contrast in response to increasing greenhouse gases. Part I: transient adjustment. *J Clim* 22:3079–3097. doi:10.1175/2009JCLI2652.1
- Edwards JM, Slingo A (1996) Studies with a flexible new radiation code. I: choosing a configuration for a large-scale model. *Q J R Meteorol Soc* 122:689–719
- Ellingson RG, Ellis J, Fels S (1991) The intercomparison of radiation codes used in climate models: long wave results. *J Geophys Res* 96:8929–8953
- Gregory JM, Webb MJ (2008) Tropospheric adjustment induces a cloud component in CO<sub>2</sub> forcing. *J Clim* 21:58–71
- Hansen J, Sato M, Ruedy R, Nazarenko L, Lacis A, Schmidt GA, Russell G, Aleinov I, Bauer M, Bauer S, Bell N, Cairns B, Canuto V, Chandler M, Cheng Y, Del Genio A, Faluvegi G, Fleming E, Friend A, Hall T, Jackman C, Kelley M, Kiang N, Koch D, Lean J, Lerner J, Lo K, Menon S, Miller R, Minnis P, Novakov T, Oinas V, Perlwitz Ja, Perlwitz Ju, Rind D, Romanou A, Shindell D, Stone P, Sun S, Tausnev N, Thresher D, Wielicki B, Wong T, Yao M, Zhang S (2005) Efficacy of climate forcings. *J Geophys Res* 110:D18104. doi:10.1029/2005JD005776
- Hasumi H, Emori S (2004) K-1 coupled model (MIROC) description. K-1 technical report. Center for Climate System Research, the University of Tokyo, p 34. Available at <http://www.ccsr.u-tokyo.ac.jp/kyosei/hasumi/MIROC/tech-repo.pdf>
- Kamae Y, Watanabe M (2012a) Tropospheric adjustment to increasing CO<sub>2</sub>: its timescale and the role of land–sea contrast. *Clim Dyn*. doi:10.1007/s00382-012-1555-1
- Kamae Y, Watanabe M (2012b) On the robustness of tropospheric adjustment in CMIP5 models. *Geophys Res Lett* 39:L23808. doi:10.1029/2012GL054275
- Klein SA, Hartmann DL (1993) The seasonal cycle of low stratiform clouds. *J Clim* 6(8):1587–1606
- Nakajima T, Tsukamoto M, Tsushima Y, Numaguti A, Kimura T (2000) Modeling of the radiative process in an atmospheric general circulation model. *Appl Opt* 39(27):4869–4878
- Ogura T, Emori S, Webb MJ, Tsushima Y, Yokohata T, Abe-Ouchi A, Kimoto M (2008a) Towards understanding cloud response in atmospheric GCMs: the use of tendency diagnostics. *J Meteorol Soc Jpn* 86(1):69–79
- Ogura T, Webb MJ, Bodas-Salcedo A, Williams KD, Yokohata T, Wilson DR (2008b) Comparison of cloud response to CO<sub>2</sub> doubling in two GCMs. *SOLA* 4:29–32. doi:10.2151/sola.2008-008
- Randall DA, Wood RA, Bony S, Colman R, Fichefet T, Fyfe J, Kattsov V, Pitman A, Shukla J, Srinivasan J, Stouffer RJ, Sumi A, Taylor KE (2007) Climate models and their evaluation. In: Solomon S, Qin D, Manning M, Chen Z, Marquis MC, Averyt KB, Tignor M, Miller HL (eds) *Climate change 2007: the physical science basis. Contribution of working group I to the fourth assessment report of the Intergovernmental Panel on Climate Change*. Cambridge University Press, Cambridge and New York, pp 589–662
- Rodwell MJ, Palmer TN (2007) Using numerical weather prediction to assess climate models. *Q J R Meteorol Soc* 133:129–146. doi:10.1002/qj.23
- Sekiguchi M, Nakajima T (2008) A k-distribution-based radiation code and its computational optimization for an atmospheric general circulation model. *JQSRT* 109:2779–2793
- Soden BJ, Broccoli AJ, Hemler RS (2004) On the use of cloud forcing to estimate cloud feedback. *J Clim* 17:3661–3665

- Taylor KE, Williamson D, Zwiers F (2000) The sea surface temperature and sea-ice concentration boundary conditions for AMIP II simulations, PCMDI Report No. 60, Program for Climate Model Diagnosis and Intercomparison, Lawrence Livermore National Laboratory, Livermore, California, p 25
- Taylor KE, Stouffer RJ, Meehl GA (2009) A summary of the CMIP5 experiment design. Available at [http://cmip-pcmdi.llnl.gov/cmip5/experiment\\_design.html](http://cmip-pcmdi.llnl.gov/cmip5/experiment_design.html)
- Watanabe M, Suzuki T, O'ishi R, Komuro Y, Watanabe S, Emori S, Takemura T, Chikira M, Ogura T, Sekiguchi M, Takata K, Yamazaki D, Yokohata T, Nozawa T, Hasumi H, Tatebe H, Kimoto M (2010) Improved climate simulation by MIROC5: mean states, variability, and climate sensitivity. *J Clim* 23:6312–6335
- Watanabe M, Shiogama H, Yoshimori M, Ogura T, Yokohata T, Okamoto H, Emori S, Kimoto M (2012) Fast and slow timescales in the tropical low-cloud response to increasing CO<sub>2</sub> in two climate models. *Clim Dyn* 39:1627–1641. doi:10.1007/s00382-011-1178-y
- Webb MJ, Lock AP (2012) Coupling between subtropical cloud feedback and the local hydrological cycle in a climate model. *Clim Dyn* doi:10.1007/s00382-012-1608-5
- Webb MJ, Lambert FH, Gregory JM (2013) Origins of differences in climate sensitivity, forcing and feedback in climate models. *Clim Dyn* 40:677–707. doi:10.1007/s00382-012-1336-x
- Williams KD, Brooks ME (2008) Initial tendencies of cloud regimes in the Met Office Unified Model. *J Clim* 21:833–840. doi:10.1175/2007JCLI1900.1
- Williamson DL, Boyle J, Cederwall R, Fiorino M, Hnilo J, Olson J, Phillips T, Potter G, Xie SC (2005) Moisture and temperature balances at the Atmospheric Radiation Measurement Southern Great Plains Site in forecasts with the Community Atmosphere Model (CAM2). *J Geophys Res* 110:D15S16. doi:10.1029/2004JD005109
- Wood R, Bretherton CS (2006) On the relationship between stratiform low cloud cover and lower tropospheric stability. *J Clim* 19:6425–6432
- Wyant MC, Bretherton CS, Blossey PN (2009) Subtropical low cloud response to a warmer climate in a superparameterized climate model. Part I: regime sorting and physical mechanisms. *J Adv Model Earth Syst* 1(7). doi:10.3894/JAMES.2009.1.7
- Wyant MC, Bretherton CS, Blossey PN, Khairoutdinov M (2012) Fast cloud adjustment to increasing CO<sub>2</sub> in a superparameterized climate model. *J Adv Model Earth Syst* 4:M05001. doi:10.1029/2011MS000092
- Zelinka MD, Klein SA, Hartmann DL (2012) Computing and partitioning cloud feedbacks using cloud property histograms. Part I: cloud radiative kernels. *J Clim* 25:3715–3735. doi:10.1175/JCLI-D-11-00248.1
- Zelinka MD, Klein SA, Taylor KE, Andrews T, Webb MJ, Gregory JM, Forster PM (2013) Contributions of different cloud types to feedbacks and rapid adjustments in CMIP5. *J Clim* 26:5007–5027. doi:10.1175/JCLI-D-12-00555.1
- Zhang M, Bretherton CS (2008) Mechanisms of low cloud-climate feedback in idealized single-column simulations with the Community Atmospheric Model, version 3 (CAM3). *J Clim* 21:4859–4878. doi:10.1175/2008JCLI2237.1
- Zhang M, Bretherton CS, Blossey PN, Bony S, Briant F, Golaz JC (2012) The CGILS experimental design to investigate low cloud feedbacks in general circulation models by using single-column and large-eddy simulation models. *J Adv Model Earth Syst* 4:M12001. doi:10.1029/2012MS000182